

Article

Assessing the Performance of In-Stream Restoration Projects Using Radio Frequency Identification (RFID) Transponders

Bruce MacVicar ^{1,*}, Margot Chapuis ², Emma Buckrell ³ and André Roy ⁴

¹ Department of Civil and Environmental Engineering, University of Waterloo, 200 University Avenue West, Waterloo, ON N2L 3G1, Canada

² Department of Geography, University of Nice-Sophia Antipolis, Provence-Alpes-Côtes d’Azur, Nice 06103, France; E-Mail: margot.chapuis@unice.fr

³ Department of Geography, Vancouver Campus, University of British Columbia, 1984 West Mall, Vancouver, BC V6T 1Z2, Canada; E-Mail: buckrell@alumni.ubc.ca

⁴ Faculty of Arts and Science, Concordia University, 1455 De Maisonneuve Blvd. W., Montreal, QC H3G 1M8, Canada; E-Mail: andreg.roy@concordia.ca

* Author to whom correspondence should be addressed; E-Mail: bmacvicar@uwaterloo.ca; Tel.: +1-519-888-4567 (ext. 38897); Fax: +1-519-888-4349.

Academic Editor: Thorsten Stoesser

Received: 21 August 2015 / Accepted: 8 October 2015 / Published: 15 October 2015

Abstract: Instream channel restoration is a common practice in river engineering that presents a challenge for research. One research gap is the development of monitoring techniques that allow for testable predictions of sediment transport and supply. Here we use Radio Frequency Identification (RFID) transponders to compare the short-term (1-year) sediment transport response to flood events in a restored and a control reach. The field site is Wilket Creek, an enlarged creek in a fully urbanized catchment without stormwater management control in Toronto, Ontario. The responses to three flooding periods, each of which are at or above the design bankfull discharge, are described. Key results are that (i) particle mobility is lower in the restored reach for all three periods; (ii) full mobility occurs in the control reach during the first two floods while partial mobility occurs in the restored reach; and (iii) the constructed morphology exerted a controlling influence on particle entrainment, with higher mobility in the pools. Log-transformed travel distances exhibit normal distributions when grouped by particle size class, which allows a statistical comparison with power law and other predictive travel-distance relations. Results show that three bedload transport conditions can occur, with partial mobility associated with a

mild relation between particle size and travel distance and full mobility associated with either a flat or steep relation depending on the degree of integration of particles in the bed. Recommendations on seeding strategy and sample sizes are made to improve the precision of the results by minimizing confidence intervals for mobility and travel distances. Even in a short term study, the RFID sediment tracking technique allows a process-based assessment of stream restoration outcomes that can be used to justify the instream intervention and plan future attempts to stabilize and enhance the system.

Keywords: stream restoration; sediment tracking; monitoring; rivers; RFID transponders; sediment transport; particle mobility; travel distances

1. Introduction

Stream restoration refers to a wide range of manipulations of streams and their riparian corridors that are intended to improve the condition of the river relative to some degraded state [1,2]. Instream structures such as artificial pools and riffles are commonly used for stream restoration projects due to their perceived benefits for ecology and channel stability [3,4]. However, the practice suffers from a lack of standards and design criteria [5,6]. Project evaluation is needed for adaptive management and progress in engineering practice [7,8], but monitoring is typically ineffective due to relatively short term monitoring projects that miss potential adjustments to relatively rare flood events, a reluctance to include the additional cost, and a tendency to collect qualitative data rather than quantitative data [9–12]. Urban streams represent a particularly acute problem due to well-known hydrologic changes and intersections with human-built infrastructure that make them a common but challenging target for restoration [13,14]. Reliable, cost effective, and repeatable techniques are needed to assess stream restoration outcomes.

Hydraulic models and laboratory studies are commonly applied to the assessment of stream restoration design hydraulics. Models of widely ranging sophistication are available, with many examples of steady-state 2D and 3D models applied to as-built designs [15–19], and Large Eddy Simulation (LES) applied to the resolution of turbulence around isolated or idealized examples of in-stream structures [20,21]. Morphodynamic models are increasingly applied to predict channel evolution in the area surrounding implemented in-stream structures [22,23], and many laboratory studies have been carried out for this purpose [24–29]. Despite the increasing sophistication, however, physical and numerical models are predictive in nature, and reliable quantitative monitoring techniques are still needed to understand project outcomes.

In the field, restoration success or failure is often assessed by measuring bed topography or geometry, for example by determining channel enlargement ratios [30], measuring local scour [28,31], or by assessing the structural integrity of restoration designs [10,32–34]. Results are notoriously difficult to compare, however, due to the time it takes for “success” or “failure” to manifest [12] and the occurrence of both positive and negative consequences that may or may not have been part of the design [34]. In fact, the reliance on geometry for the evaluation of restoration outcomes imposes a static ideal for morphological trajectories that runs counter to fluvial geomorphic principles of dynamic

equilibrium. Although absolute channel stability may be part of the design for some restoration projects, most rivers have an alluvial component such that channel erosion and deposition are necessary for the maintenance of sedimentary bedforms, long-term stability, and ecosystem function [2,35,36].

The science of bedload transport in rivers currently relies on a number of indices and metrics of sedimentary behavior to compare different reaches. For instance, a number of studies in mixed-gravel beds have demonstrated the prevalence of partial mobility [37–40], and characterized the relation between particle size and travel distance [41–43]. Tracking methods using Radio Frequency Identification (RFID) transponders have become common in the research community due to their advantages over other tracking technologies in terms of individualized particle displacement information, low cost, battery-free nature and robust design [44–51]. Sediment tracking has been used to assess some restoration projects [52–54] but its potential for testable hypotheses to assess restoration outcomes has yet to be fully realized.

The aim of this study is to develop and test a strategy for assessing stream restoration outcomes through the use of sediment tracking data. This aim is a direct response to Wilcock's [2] challenge for the research community to develop robust methods that produce meaningful and testable predictions of sediment transport and supply that could be used for restoration design. Statistical tests are described that assess particle mobility and compare travel distance distributions in an urban creek in sections with and without instream restoration. The described method is suited to gravel-bed rivers with active layers that are less than the detection range of the system (~0.30 m [55]). The widespread application of this method would help to bridge the gap between the science of fluvial geomorphology and restoration design.

2. Methods

2.1. Field Site

Wilket Creek is a tributary of the Don River in the City of Toronto with a drainage area of 15.4 km² (Figure 1). The watershed is underlain by the Halton Plain Till, a predominantly clayish cohesive till. The creek profile cuts down through layers of glacial deposits with varying quantities of clay, silt, gravel and coarser materials that supply a mixed load to the creek. Current land surface cover is dominated by suburban residential areas with some commercial and higher intensity uses in the upper watershed. The conversion from agricultural to urban land uses occurred in the 1950s and 1960s as the City of Toronto expanded rapidly. The land use change resulted in many modifications to the drainage patterns that are typical of urbanization, including increased imperviousness and more rapid routing of surface runoff.

Wilket Creek itself was converted to a storm sewer in the upstream part of its catchment, leaving only about 6 km of open channel (Figure 2). A riparian parkland was also left through the open channel portion of the creek and is now heavily used for recreation, with a number of bridge crossings. A sanitary trunk sewer was routed through the valley during the urban expansion, which resulted in the channel being straightened in many locations. Erosion is endemic in the river corridor, with channel enlargement and incision leading to bridge failures and exposure of the sewer where its route intersects with that of the river. Measures such as gabion baskets (wire baskets filled with stone), riprap (angular

quarried stone), and armourstone (large $1 \times 0.5 \times 0.5$ m limestone blocks) have been extensively used, but the failures of such measures can be readily observed along the creek. Massive erosion during floods in 2005 and 2008 led to the development of a new management plan for the lower 3 km of the channel [56] and restoration of a 300 m long section in 2011 that was monitored in this study.

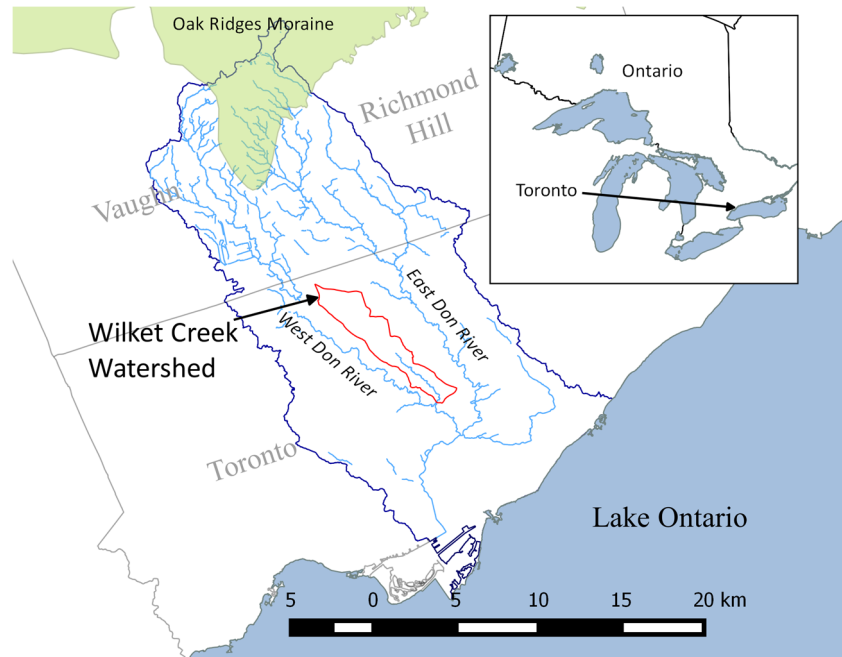


Figure 1. Geographical context of the Wilket Creek watershed. GIS layers were provided by the Toronto Region Conservation Authority.

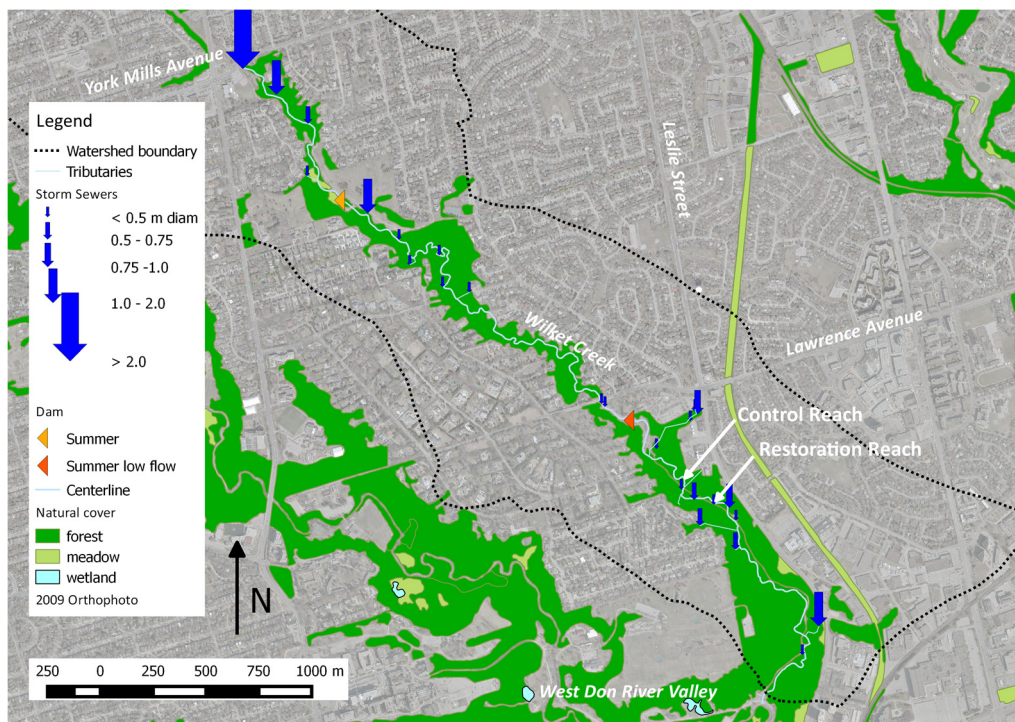


Figure 2. Open channel section of Wilket Creek including locations of control and restoration study reaches. The natural cover GIS layer was provided by the Toronto Region Conservation Authority.

The restoration approach involved the construction of coarse riffle-pool sequences through an irregularly meandering channel (Figure 3). This approach was chosen to roughly match with riffle-pool morphology in the rest of the creek while dissipating energy and working around constraints posed by existing infrastructure [56]. Constructed riffles were coarser than the rest of the creek as they used quarried angular material and buried lines of stones greater than 1 m in diameter to fix bed elevations over sanitary sewer crossings. Given the coarse bed material and the relatively high slope of the channel through the restoration section ($S_o = 1.12\%$), these structures could also be considered morphologically analogous to cascades with intervening pools. Angular stone was terraced on the banks and vegetation was planted between terraces to enhance long-term stability. The channel dimensions of the restored section were set to match the anticipated size of the urbanized channel. Using the concept of critical velocity, the consultants forecast that the ultimate stable channel width that would account for the change in hydrology as a result of urbanization within the watershed is equal to 13 m [56], which is approximately three times the pre-urbanization width but only slightly larger than the existing top-of-bank width of 10–12 m [57]. Riffles and pools were designed to have bankfull depths of 1.0 m and 1.5 m, respectively [56].



Figure 3. Photograph of restoration site July 2013, approximately 18 months after construction. Note the rocky riffle upstream of the pool in the middle of the frame and the point bar largely formed from deposited sand and gravel. Flow is from top to bottom.

2.2. Field Methods

Standard methods were used to measure topographical and sedimentological information about the site. A centerline profile of the channel and channel cross-sections were measured to help understand particle displacements and their relation to channel morphology. A total of 18 cross-sections were established and additional points were added at slope breaks and within the floodplain following the recommendations by Heritage *et al.* [58]. A digital elevation model (DEM) was created from this data using linear interpolation between data points. Wolman pebble counts within the restored and the

upstream control sections were completed to characterize the surface bed material (Figure 4). A minimum of 200 particles >5 mm in diameter were counted, with the number of fine particles and clay till exposures also recorded. A pebble count with 100 stones completed by the consultant prior to the restoration construction was used for comparison [56]. The estimated D_{50} for the entire bed surface ranges between 58 mm for the control reach and 115 mm for the restored reach. Approximately 22% of the bed surface is covered with sand while 7% of the bed surface is exposing the cohesive till. If the finer material is included, the median grain size in the control reach is approximately 40 mm.

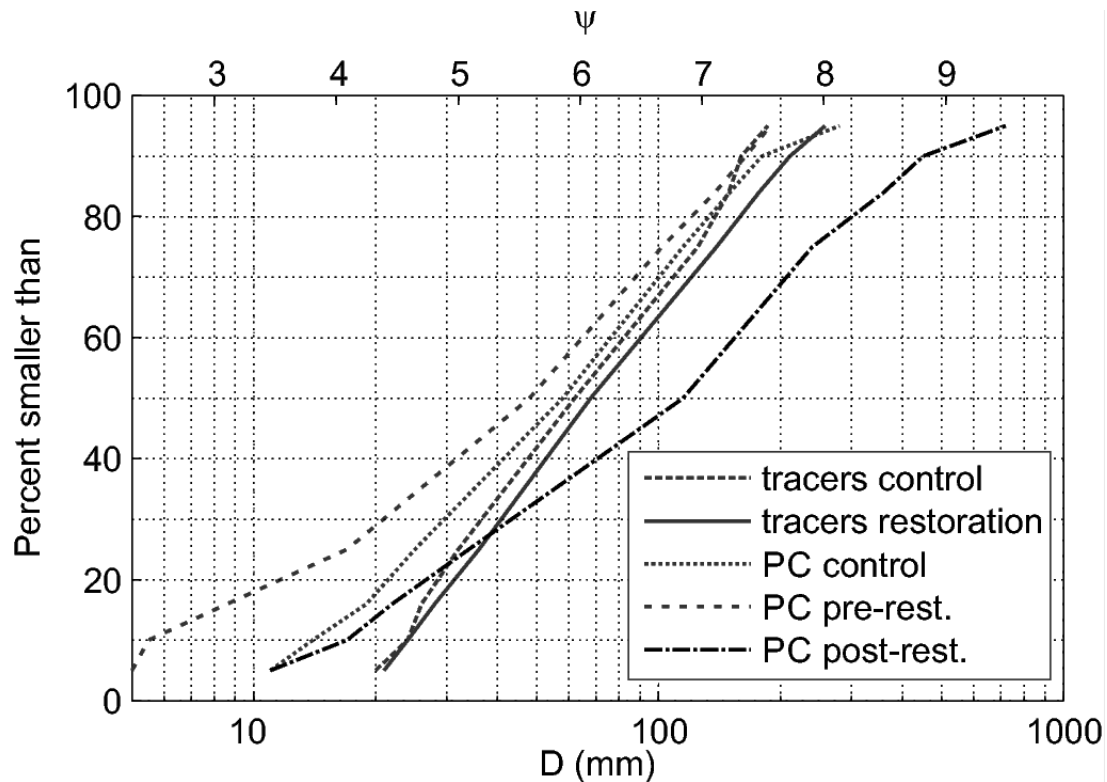


Figure 4. Particle size distributions of tracers populations and bed sediment samples (pebble counts—PC) in the control and restoration reaches. Pre-restoration information was completed by Parish Geomorphic [56].

Two pressure gauges and one barometric gauge were installed at the restoration site to record water surface elevations. The instream stations consisted of steel pipes with drilled holes, two sizes of metal screen wrapped and welded around the pipe, a drive point tip, and a bolted cap. Gauges were hung from a wire attached to the cap so that they were suspended below the bed in order to ensure the continuous measurement of low water levels. The screens prevented the majority of sediment from coming in, although it was found necessary to pump out the material using a custom built hand pump in the summer of 2014. The gauges were Hobo™ U20 water level loggers with a calibrated accuracy of ± 3 mm and a range of 0–4 m. Gauge data were downloaded periodically and corrected for atmospheric variations with the barometric gauge. Gauges were set to measure pressure at a one minute interval during the summer and a five minute interval during the winter. Through the winter the upstream gauge was removed due to the possibility that it would be damaged as a result of freezing. The downstream gauge was left in as a test and was found to have functioned normally throughout this

period. Due to poorly defined rating curves, the gauge data was used to estimate shear stress but not discharge.

A range of particle sizes were tagged to characterize bed material dynamics within the channel. The size distribution largely followed the size distribution in the control reach upstream of the restored section (Figure 4). The ψ scale as defined in Parker [59] was used to delineate particle size classes ($D = 2^\psi$ where D denotes particle size in mm). The tagging procedure consisted of collecting the rocks from the site, drilling a small hole for the tag, inserting the tag and then protecting and securing the tag by filling the remaining space within the drilled hole with a masonry caulking. Tagged particles were measured, weighed, and their volume was determined using water displacement. It was not possible to use either the very small stones due to the minimum size of the tags or the very large stones due to the difficulty of bringing large stones back to the lab for the tagging procedure. Large angular stones (>128 mm or 7ψ) used for the riffles in the restoration reach were tagged in the field. Only the intermediate axis of these stones was estimated as they were sometimes buried within the bed. Larger RFID transponders were used as the size of the stone permitted so that 12 mm (model # TRPGR30TGC), 23 mm (model #RI-TRP-WR3P) and 32 mm (model # RI-TRP-WR2B) transponders were used in the $<5 \psi$, $5-6 \psi$, and $>6 \psi$ size classes, respectively.

In total, 300 tracers were seeded on the restored site and 143 tracers were seeded on the upstream control site (a second control site with ~ 150 tracers had to be abandoned due to excessive lateral mobility and emergency restoration works). At each seeding site, approximately 10 tracers were spaced ~ 1 m apart on a cross-section, with the total number of sections depending on the total number of tagged particles in the respective reaches. The tracers were placed on the surface of the bed and randomized based on particle size. The surface placement allowed us to isolate the effect of fluid shear stress in the initial mobilization of the particles, but will tend to overestimate mobility and travel distances relative to the rest of the bed particles. The size randomization ensured that all particle sizes were represented in all areas of the bed for the initial test.

Particle positions were detected using a round loop antenna manufactured by Aquartis Ltd (Quebec, Canada). The mean radius of detection for this equipment combination is between 0.05 and 0.41 m depending on the size of tag and the orientation of the tag relative to that of the antenna [55]. A conservative estimate of 1 m was used for a movement classification threshold following previous studies [45,47]. The positions of tagged particles were mapped using a total station. Between the period of August 2013 and August 2014, at least four events reached the design bankfull depth of 1.0 m (0.63 m above baseflow) at the gauge located at the upstream limit of the restoration site (Figure 5). Six surveys were completed at each site to characterize particle displacements. For the current analysis, only the flooding periods in 2014 ending on 22 May, 25 July and 21 August were included (Table 1). Smaller floods prior to the 22 May date did not result in significant mobility and the data were aggregated with the 22 May survey. All three flooding periods had dimensionless shear stress values that are close to a threshold value ($\tau_c^* \sim 0.047$ from [60]) in the restoration reach but in the order of $\sim 2\tau_c^*$ in the control reach.

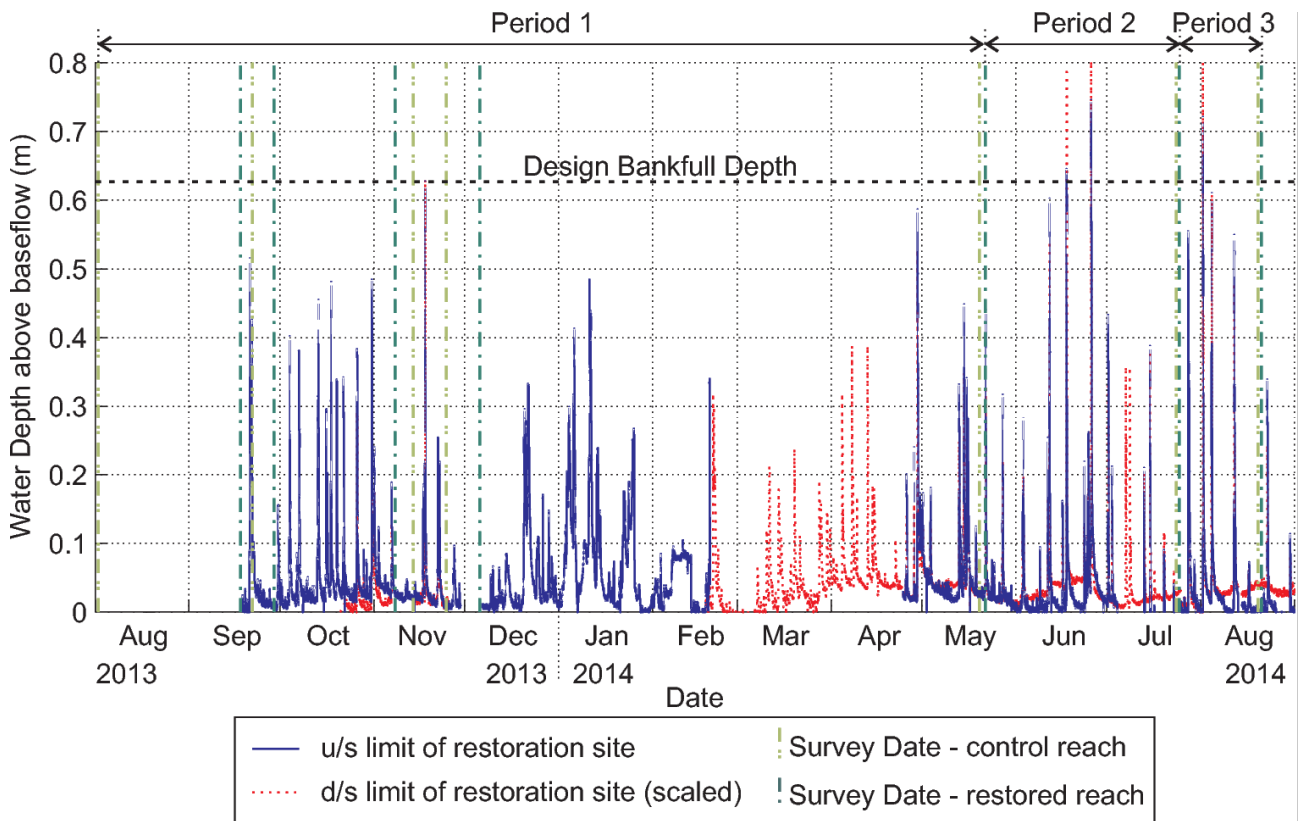


Figure 5. Water surface elevation above baseflow at the upstream limit of the restoration reach. Water surface elevations above baseflow at the downstream limit of the restoration site were scaled to illustrate the degree of flooding in two periods where the upstream gauge was not active. Note that water surface elevations could not be obtained from 1 August 2013 to 18 September 2013 due to an error with the barometric gauge. All survey dates are indicated as are the periods used in the current paper for analysis.

Table 1. Floods and sampling period. Note that the start date for flooding period 1 was later for the restoration reach than the control reach, but no significant flood occurred in the intermediate period. Depth (Y) and shear stress (τ) values are the maximum values within the study period. Dimensionless shear stress values ($\tau^* = \tau / ((\rho_s - \rho)gD_{50})$) are calculated using the D_{50} in the control reach (58 mm) and in the post-construction restoration reach (115 mm). For reference, the bankfull depth in the control reach is 0.87 m and the design bankfull depth in the restoration reach is 1.0 m.

Period	1	2	3
Start date	August/September 2013	22 May 2014	25 July 2014
End date	22 May 2014	25 July 2014	21 August 2014
Maximum flood date	18 November 2013	25 June 2014	1 August 2014
Y (m)	1.01	1.13	1.11
τ (N/m ²)	80	90	88
τ^* ($D_{50} = 58$ mm)	0.085	0.094	0.097
τ^* ($D_{50} = 115$ mm)	0.043	0.048	0.047

2.3. Data Analysis

2.3.1. Mobility

Particle mobility (\hat{p}_m) is defined as the percentage of particles that are displaced in a given flood (note that the symbol $\hat{}$ is used to denote the entire population of tracers). For each flood, the sample mobility (p_m) was calculated as:

$$p_m = \frac{n_m}{n_{fb}} \quad (1)$$

where n_{fb} is the number of particles that were found (or whose positions could be inferred) at both the beginning and the end of the survey period, and n_m is the number of found particles that moved. Positions were inferred where particles were not found in the survey at the end of the period but were found in a more recent survey and determined to have remained immobile throughout.

To determine whether the restoration has a significant effect on \hat{p}_m , it is necessary to estimate the precision of the samples (p_m). Confidence intervals for \hat{p}_m can be estimated from binomial statistical techniques based on the principle that, if it can be assumed that samples are independent and random, repeated samples should yield a normal distribution of success probability [61]. Stated mathematically, the standard error of \hat{p}_m can be calculated as:

$$SE(\hat{p}_m) = \sqrt{\hat{p}_m(1 - \hat{p}_m)/n_{fb}} \quad (2)$$

and the z-scores of p_m will have an approximately normal distribution:

$$z = \frac{p_m - \hat{p}_m}{SE(\hat{p}_m)} \quad (3)$$

If we can further assume that:

$$SE(p_m) \approx SE(\hat{p}_m) \quad (4)$$

which is commonly done [61], then:

$$\hat{p}_m = p_m \pm z_{\alpha/2} SE(p_m) \quad (5)$$

where $z_{\alpha/2}$ can be determined from standard tables for the normal distribution for a given confidence level (α).

In most gravel bed rivers, partial transport is dominant [39,40]. This condition is highly desirable in restored reaches because it indicates that the larger particle sizes are less mobile than the smaller size, which means that they are likely to provide some structural stability during a flood event, even if the smaller size material is mobilized. The occurrence of partial mobility can be detected by a negative relation between mobility and particle size. To determine whether such a trend was present in a given reach during a flooding period, we used the runs test [62]. This non-parametric test is widely applied in a variety of fields [63,64] due to its suitability for the determination of trends in binary data such as particle mobility. Critically, it is not necessary for the binary results to have equal probabilities of occurring. In the test, the number of elements is defined as N , and a run is defined as a continuous sequence of elements either above (N^+) or below (N^-) a calculated mean (\bar{N}) in the series. The

principle of the test is that the number of runs is a random variable whose distribution is approximately normal. From Wald and Wolfowitz [62], \bar{N} is calculated as:

$$\bar{N} = 1 + \frac{2N^+N^-}{N} \quad (6)$$

and the variance (σ_N^2) is:

$$\sigma_N^2 = \frac{(\bar{N}-1)(\bar{N}-2)}{N-1} \quad (7)$$

If the number of runs is higher or lower than a given confidence interval determined with a z-score, then the elements are not randomly distributed and the hypothesis of a stationary series is rejected. In terms of mobility, a negative result indicates that partial mobility occurred during the flood.

2.3.2. Travel Distance

Travel distance was assessed by grouping the particles by size class and comparing mean travel distances to the relation proposed by Church and Hassan [41] for travel distances in a gravel bed river:

$$\frac{\bar{L}_i}{\bar{L}_{D50}} = \left(1 - \log \frac{\bar{D}_i}{D_{50}}\right)^{1.35} \quad (8)$$

where \bar{L}_i is the mean travel distance for particles in a size class i , \bar{D}_i is the corresponding mean particle size, and \bar{L}_{D50} is the geometric mean travel distance of particles in the median size class. In their discussion, Church and Hassan [41] note that Equation (8) was derived from data obtained with painted tracers for which only the first displacements of particles were available and only those particles that were visible on the bed surface. Wilcock [65] notes that Equation (8) is representative of gravel bed rivers that are partially mobile. For fully mobile particles, Wilcock [65] showed that the distribution is expected to be flatter due to the effects of particle interactions. In contrast, Church and Hassan [41] showed that unconstrained particles on the surface will follow a uniform inverse power law as:

$$\frac{\bar{L}_i}{\bar{L}_{D50}} = \frac{\bar{D}_i^{-2.0}}{D_{50}} \quad (9)$$

Confidence intervals can be drawn for \bar{L}_i using standard techniques if it can be assumed that the sample of transport distances in a given size class (L_i) is normally distributed. The Kolmogorov-Smirnov test was used to test both the absolute transport distances and the log-transformed travel distances for this purpose ($\alpha = 0.05$). In order to demonstrate the application of the test, log-transformed travel distance histograms for the May 2014–July 2014 period are shown in Figure 6. Normal distributions are evident for the 4–5 ψ and the 7–8 ψ size classes. The other distributions appear somewhat skewed (6–7 ψ) or even bi-modal (5–6 ψ), but in all cases the hypothesis of a normal distribution was not rejected with the Kolmogorov-Smirnov test. Similar results were found for the travel distance distributions of both reaches and all flooding periods in this study. The hypothesis of normality was frequently rejected for travel distance distributions where no log transform was applied, as it was where null travel distances were included.

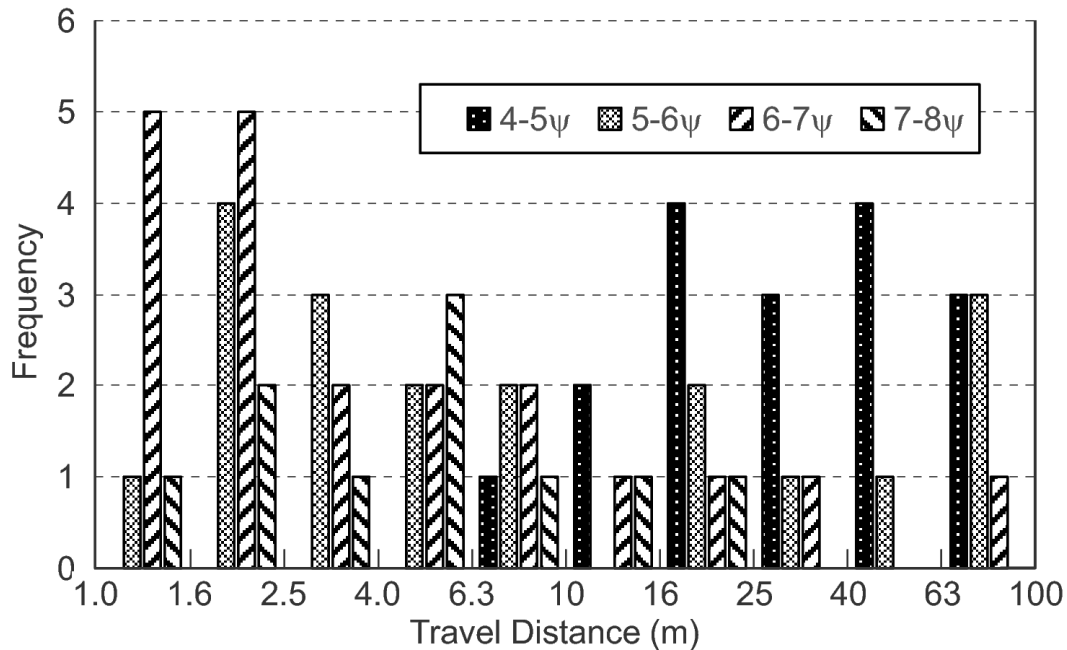


Figure 6. Histograms of log-transformed travel distances by size class for the largest flood (May 2014–July 2014) in the restoration reach.

3. Results

3.1. Basic Particle Tracking Statistics

Statistical analysis of tracer movement during a flooding period requires the definition of the subset of the total population of particles that can be used in the analysis. As noted by Schneider *et al.* [48], it is not enough to report single survey recovery rates because particles must be found in both the pre- and post-flood surveys to be useable. The quality of all surveys in the current study was high, finding between 87% and 92% of the tagged particles in each site, but the intersection of the found particles in the pre- and post-flood surveys is lower in the second and third flooding periods (Table 2). Schneider *et al.* [48] also distinguished particles that were lost (*i.e.*, were not found in subsequent surveys— n_{lost}) from those that were merely missing and later “re-emerged” (*i.e.*, were found in subsequent surveys). Here we note that some positions of missing particles can be inferred (n_{inf}) if they were found in a more recent survey and determined to have remained immobile throughout, which means that they can be added to the tally of particles that were located (n_l) to get a total number of “found” particles (n_f). Missing particles that did move in subsequent surveys ($n_{missing}$) and those that were not found in any subsequent survey (n_{lost}) could not be utilized for statistical analysis. Future surveys may change these numbers by shifting some lost particles to the inferred and missing classes. In August 2014, lost particles accounted for about 10% of the total, with a higher proportion in the restored reach (Table 2). In the control reach, particles that moved out of the reach were recovered in the restoration reach, including five particles during the May–July 2014 flooding period, which accounts for the difference in the rate of lost particles between the reaches.

Differences in overall particle mobility (p_m) show the effect of flood magnitude and antecedent floods on sediment dynamics. In all cases, p_m is higher in the control reach (Table 2). Minor overlap of the confidence intervals (CI_{p_m} ; $\alpha = 0.05$) is noted for the second and third floods for the restored and

control reaches. p_m is highest in the first flood in the control reach ($p_m = 0.56 \pm 0.09$) but highest in the second and largest flood in the restoration reach ($p_m = 0.30 \pm 0.06$). For both the control and the restored reaches, the mobility appears to decrease with subsequent floods, as p_m is significantly lower in the third flood as compared to the first flood, despite the higher peak magnitude of the flooding in the third period. Reduced mobility of tracers is expected from previous studies [50,66], particularly where the initial particles are seeded loosely on the bed of the channel as they were in this case.

Table 2. Particle tracking statistics for the three flooding periods in both the control and restoration reaches, where n_t is the total number of particles present in the reach, n_l is the number located in the survey, n_{inf} is the number of inferred particles, n_f is the number of found particles, p_f is the percentage of found particles, n_{fb} is the number of particles found in both the beginning and end surveys for each period, p_{fb} is the percentage of particles found in both surveys, n_m is the number of particles that moved, p_m is the percentage of moved particles, CI_{pm} is the confidence interval for p_m , $\overline{L_{D50}}$ is the geometric mean travel distance of the particles in the D_{50} size class that moved, CI_{D50} is the confidence interval for $\overline{L_{D50}}$, n_{D50} is the number of particles in the D_{50} size class, $n_{missing}$ is the number of particles that were not found in the current survey but which were found in a subsequent survey, n_{lost} is the number of particles that have not been found in subsequent surveys, n_{exit} is the number of particles known to have moved downstream of the reach, and n_{enter} is the number of particles known to have moved into the reach from upstream.

Flooding Period	1		2		3	
	Control	Restoration	Control	Restoration	Control	Restoration
n_t	143	300	143	300	138	305
n_l	120	244	132	257	126	267
n_{inf}	7	16	0	7	0	0
$n_f = n_l + n_{inf}$	127	260	132	264	126	267
$p_f = n_f/n_t$	0.89	0.87	0.92	0.88	0.91	0.88
$n_{fb} = n_f \cup n_f(t-1)$	127	260	122	242	122	253
$p_{fb} = n_{fb}/n_t$	0.89	0.87	0.85	0.81	0.88	0.83
n_m	71	56	55	73	28	32
$p_m = n_m/n_{fb}$	0.56	0.22	0.45	0.30	0.23	0.13
CI_{pm}	0.47–0.65	0.17–0.27	0.36–0.54	0.24–0.36	0.16–0.31	0.09–0.17
$\overline{L_{D50}}$ (m)	4.2	3.0	29	17	17	55
CI_{D50} (m)	1.7–11	1.7–5.3	12–70	5.6–52	10–30	29–100
n_{D50}	5	5	7	9	6	4
$n_{missing}$	11	25	5	14	2	0
$n_{lost} = n_t - n_f - n_{missing}$	5	15	6	22	10	38
n_{exit}	0	0	5	0	1	0
n_{enter}	0	0	0	5	0	1

Travel distance statistics also show the effect of flood magnitude and antecedent flooding, but variability was too high in many cases to derive meaningful conclusions. One significant result was that the travel distance in both reaches was lower in the first flood than in subsequent events.

Thus, while mobility was relatively high in the control reach, the particles were moving relatively short distances in this lower magnitude event. Short travel distances also were found in the restored reach. In the second flood, transport distances are higher, but the variability is too high to conclude that the restoration had an effect on travel distance. In the third flood, travel distance confidence intervals overlap with those in the second flood and slightly overlap between the reaches. The relatively small overlap (~ 1 m, or $<5\%$ of $\overline{L_{D50}}$ in the control reach) suggest that the $\overline{L_{D50}}$ might be higher in the restored reach, which was not anticipated given that the potential to induce tracer deposition is theoretically higher in the restored reach due to the wider channel, large angular riffle material, and pool-riffle morphology. Overall the results suffer from the low number of tracers in the D_{50} size class ($\psi_{D50} = 5.5\text{--}6$; $n_{D50} < 10$), and variability is quite high. For example, confidence intervals are as large as 71 m in the restored reach for the third flood period.

3.2. Spatial Results

Some of the most relevant data from a stream restoration perspective are the spatial results that show locations of entrainment and deposition. Plotted at a reach scale, the starting (August 2013) and ending (August 2014) positions of the tagged particles illustrate the degree to which the different sizes of stones moved through the restoration section (Figure 7). Smaller tracers (4–5 ψ) generally moved farther than the larger sizes. With the exception of a single stone in the 7–8 ψ size class, the tracers larger than 6 ψ did not travel far downstream of their seeding positions, while the smaller size classes moved well downstream, even reaching the end of the surveyed section by August 2014. The transported tagged particles in the smaller size fractions were deposited primarily on the inner bank (point bar) of pool 3 and near the cross-over (riffle) between pools 4 and 5.

A closer view of pools 1 and 2 shows that entrainment and deposition are a function of the riffle-pool morphology (Figure 8). For the smallest size class, the particles from the upstream riffle were nearly entirely entrained and moved downstream where they deposited on the second riffle and on the inner bank of the bends. Some of the 5–6 ψ tracers remain in the upstream riffle and show an increased tendency to deposit in the pools. In contrast with the smaller sizes, the 6–7 ψ tracers do not show widespread entrainment because nearly all of the tracer positions in August 2013 are closely associated with the positions in 2014. Localized entrainment is noted on the point bar between pools 1 and 2. Entrainment of the 7–8 ψ tracers is noted only in the pools. Overall, the 2013 positions can be visually correlated with the 2014 positions, which indicates that transport distances were short.

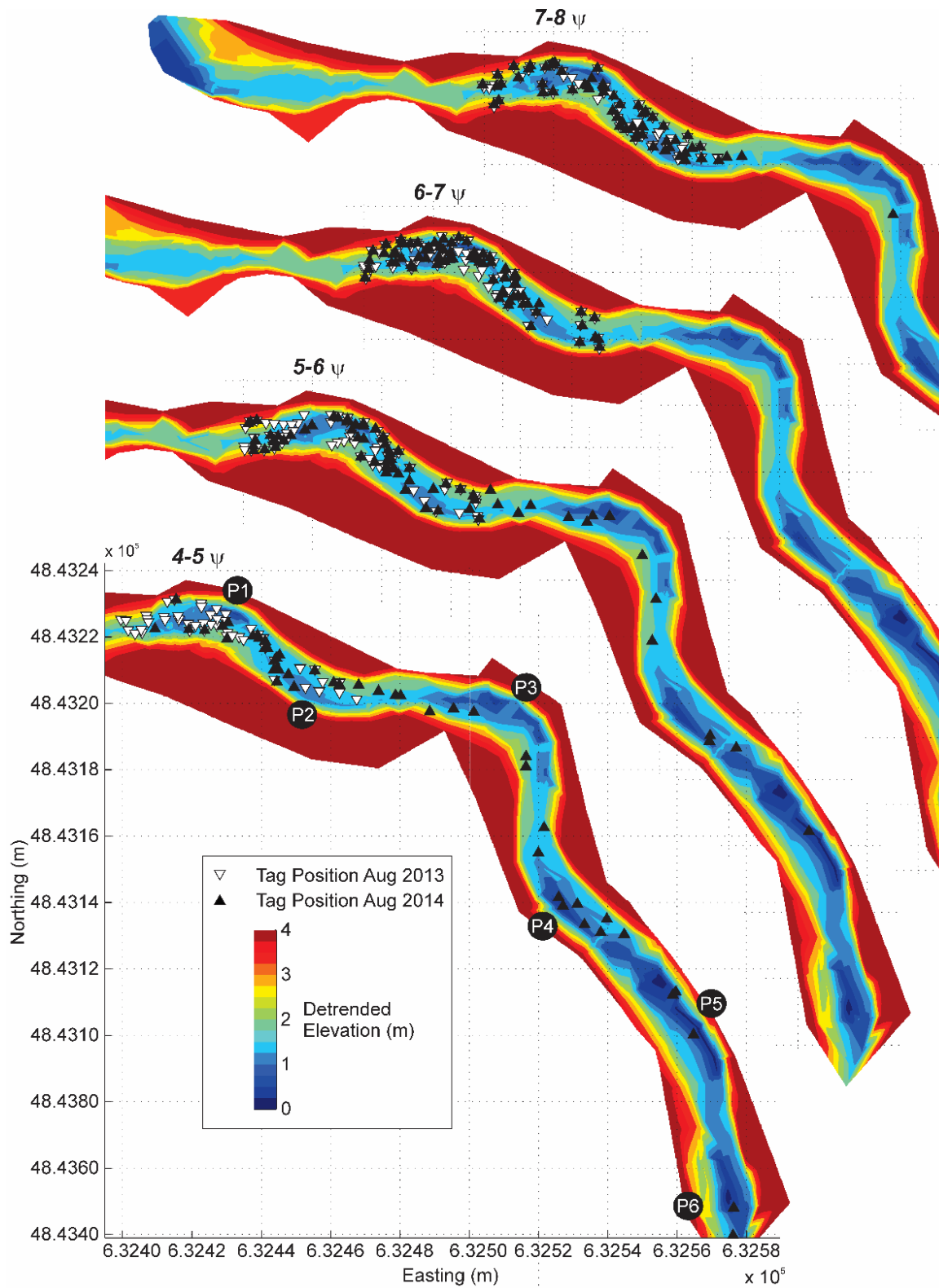


Figure 7. Entrainment and deposition through the restoration reach over 1 year of tracking. The elevation has been detrended by subtracting the overall slope ($S_o = 1.12\%$) of the channel. Grid squares are 20×20 m. Pools are numbered from upstream to downstream to facilitate the description of the results.

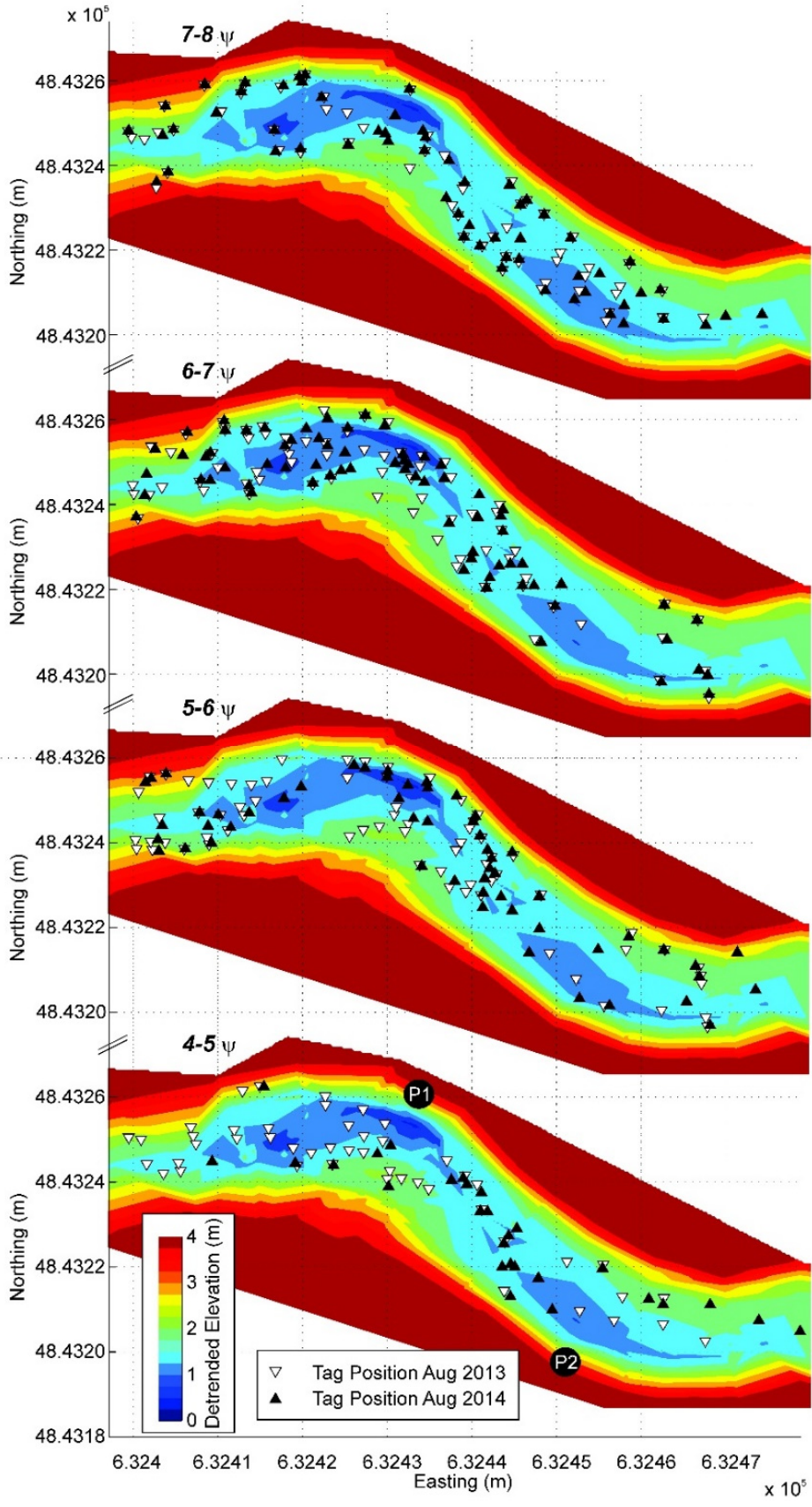


Figure 8. Entrainment and deposition over 1 year of tracking shown at morphologic sub-unit scale. The elevation has been detrended by subtracting the overall slope of the channel. Pools are numbered to facilitate the description of the results.

3.3. Mobility

The relation between particle size and mobility shows a number of important differences between the restored and the control reaches. In the initial flooding period, significantly higher mobility occurs in the control reach for particles with sizes between 5.5 and 7.5 ψ , a size range that roughly corresponds with the D_{50} to D_{84} particles (Figure 9a). No statistical differences are apparent for particles that are either smaller or larger than this range. Confidence intervals are relatively large (up to ± 0.25 of the vertical axis), which reduces the ability to statistically test hypotheses. This problem is caused by the small number of tracers in each size class. For example, in the control reach, only 20 stones per size class were seeded, and sample sizes could be much lower where particles were missing or lost. In the restored reach, the mobility was low and the samples were larger, both of which result in a lower standard error. Another key observation from the mobility of the initial flood is that a flat line can be drawn through confidence intervals for the control reach, which indicates that there is no size-dependent relation, *i.e.*, that it is fully mobile through the 8 ψ size class. In contrast, the smaller sizes ($< D_{50}$) were significantly more mobile than the larger sizes in the restored reach. A check with the runs test, however, shows that the hypothesis is accepted at $\alpha = 0.05$ (Table 3), which means the relation with size is not significant in either the control or the restored reach despite the higher mobility of the smaller sizes in the restored reach. The runs test is sensitive to the number of categories ($N_{categories}$), which is low, as it refers to the number of size classes used to assess the trend (*i.e.*, 8 or 9 classes). In the calculation, the relatively high mobility of the 6.0–6.5 ψ size class (Figure 9a) split the mobility series into more runs, which meant that the overall trend in this first flooding period was not significant. However, the error bars show that p_m of any size class is relatively uncertain and that the runs test is sensitive to sampling variability. Larger sample sizes would produce more robust results, while a Monte Carlo approach to the runs test could be used to assess the effect of sampling variability on the runs test.

Table 3. Assessment of trend in relation between mobility and particle size in control and restored reaches using the runs test [62]. The rejection of the hypothesis means that the relation between particle size and mobility is significant, which is indicative of partial mobility.

Period	1		2		3	
	Control	Restoration	Control	Restoration	Control	Restoration
$N_{categories}$	8	9	8	9	8	9
N^+	4	3	4	4	3	5
N^-	4	6	4	5	5	4
N_{runs}	4	4	5	2	3	3
\bar{N}	5	5	5	5.4	4.8	5.4
σ_N^2	1.7	1.5	1.7	1.9	1.5	1.9
Hypothesis accepted?	Y	Y	Y	N	Y	Y

In the second flood and largest flood, no significant difference in mobility is apparent between the restored and control reaches in any size class (Figure 9b). The mobility of the smaller size classes in the control reach is less than the mobility in the initial flooding period and the mobility in the restored reach, but the large error bars mean that the observed differences are not significant. The mobility is

generally higher in the control reach from D_{50} to D_{84} and also shows full instead of partial mobility. A flat line can again be drawn through the confidence intervals for the control reach up to 8ψ , which is not possible for the restored reach, and the runs test shows that there is a significant relation between particle size and mobility in the restored reach during the second flooding period (Table 3).

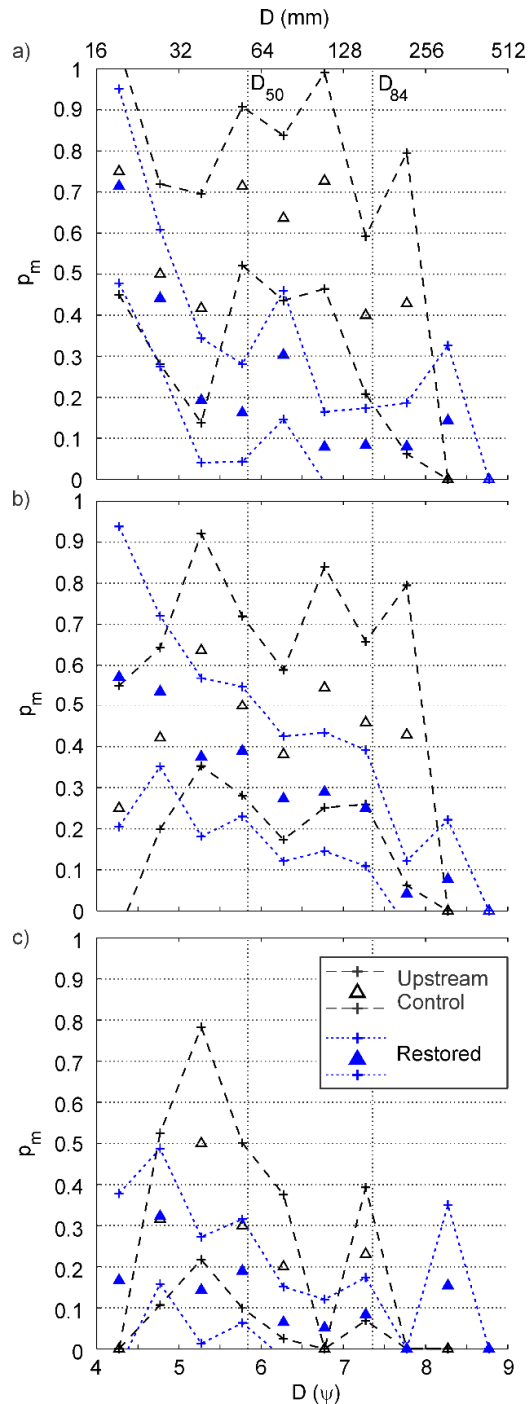


Figure 9. Mobility for upstream control and restored for time periods: (a) August 2013–May 2014; (b) May 2014–July 2014; and (c) July 2014–August 2014. 95% confidence intervals are shown as dashed and dotted lines for the upstream control and restored reach, respectively.

In the third event the particles in the control reach that are smaller than the D_{50} sizes are less mobile than the D_{50} , a trend which is not expected from the literature. The apparent reduced mobility may be a function of the use of smaller RFID transponders used for these size classes, which reduces recovery rates due to shorter detection distances, or to the travel distances observed in the previous floods, which meant that some of the highly mobile particles may have travelled downstream of the reach. A spatial search of missing particles in this size class shows that all of the small ($<5 \psi$) particles that were lost from the control reach had previously travelled more than 50 m downstream from the seeding section and half had deposited in a sedimentary bar, which indicates that both the short detection distances and travel out of the reach may have been factors.

3.4. Travel Distance

Travel distances are plotted on a normalized distance *versus* particle size plot following the method described by Church and Hassan [41] for comparison between reaches, flooding dates, and with Equations (8) and (9). The initial flooding period shows that smaller sizes tend to travel much farther than those equal to or larger than the D_{50} . Based on a comparison with the trend lines, the smaller particles fit the power law relation rather than that proposed by Church and Hassan [41]. Above the D_{50} , however, the transport distances show no significant relation with particle size or between the restored and control reaches (Figure 10). Travel distances overall are short ($\overline{L}_{D_{50}} \sim 3\text{--}5$ m), so that particles equal to or larger than the D_{50} all travel about the same distance, which is less than one channel width. The maximum water level during this first event was 10–15 cm less than the maximum observed flood.

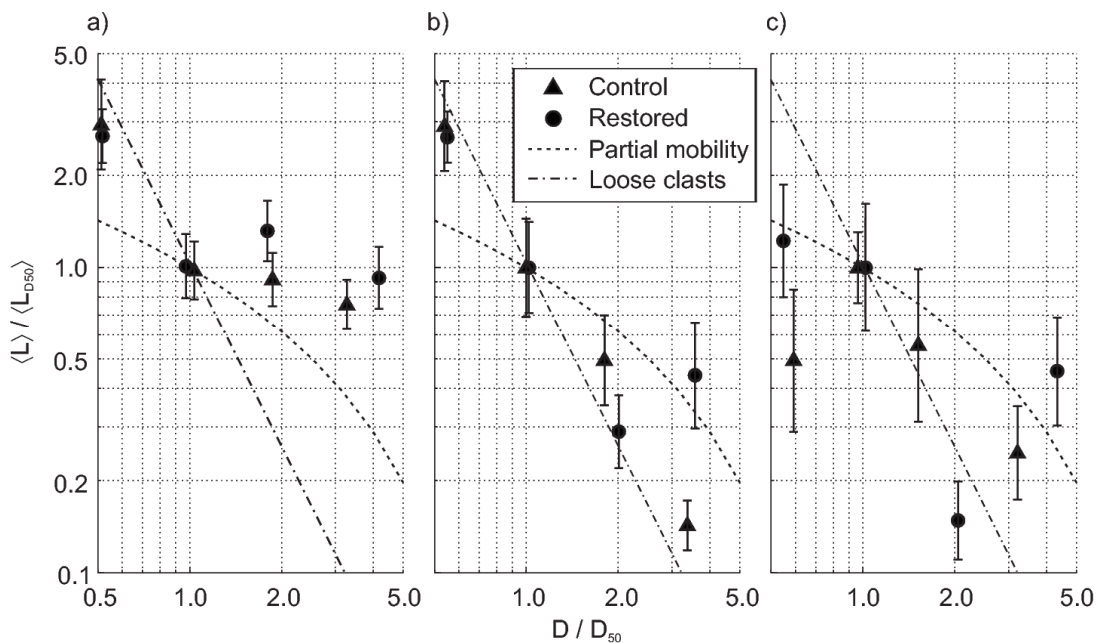


Figure 10. Travel distances in control and restored reaches for (a) August 2013–May 2014; (b) May 2014–July 2014; and (c) July 2014–August 2014. Lines representing partial mobility (Equation (8)) and transport of loose unconstrained clasts (Equation (9)) are shown for comparison.

The relation between travel distance and particle size changes as a function of the flooding period. The second and third floods have higher peak magnitudes, and travel distances are much longer overall (Table 2). In the second flood, the control reach shows a power law distribution (Equation (9)) of travel distances over the full range of tracked particle sizes (Figure 10), which is in agreement with previous studies of large magnitude floods where particles are loosely seeded [41,45]. In the third flood the relation is much closer to Equation (8), which indicates that the particles are worked into the bed and are more constrained by their neighboring clasts.

The restoration does not exert a clear influence on travel distances (Figure 10). In the second flood, mobile particles in the largest size class tend to travel relatively far in the restored reach in comparison with the control reach, but otherwise the results follow Equation (9) and are not significantly different from the control reach. In the third flood the relation is again much closer to Equation (8) as was observed for the control reach, but the third particle size class seems to follow Equation (9). It is not clear from the travel distance plot alone what the reason could be behind such behavior, although the spatial plots show that these particles tend to become trapped in the riffle and the pool tail (Figure 8). The trapping may thus be a result of larger particles and pore spaces in the restored riffle sections, indicative of size sorting due to the restoration approach, or variability that is insufficiently quantified due to the relatively low numbers of tracers.

4. Discussion

An explicit assumption in the commissioning of many restoration projects aimed at arresting channel incision or protecting infrastructure is that the design will increase bed stability. In Wilket Creek, converging evidence indicates that the design is succeeding in this regard. First, a difference is shown in overall particle mobility between the restored and control reach that is significant for two of the three flooding periods and just missing on the third (Table 2). Second, results from the spatial displacements show that the larger particles in the riffle are rarely displaced in the restored reach and, if they do move, it is over short distances (*i.e.*, less than one channel width; Figure 8). Partial mobility is also confirmed in the largest event for the restored reach during which full mobility occurs in the control section (Table 3). Full mobility is particularly dangerous in a system like Wilket Creek's, because the largest material is typically glacial lag from bank erosion, a source that is increasingly restricted due to bank protection measures. Other sources of gravel material such as tributaries and the upstream catchment have largely been replaced with storm sewers, meaning that the supply of coarse material is less than in the historical condition. When glacial lag material is moved, steps and riffles disappear and glacial till is increasingly exposed on the stream bed (for example, after the floods in 2014), which confirms that the channel continues to incise where it has not been restored. Significantly for monitoring restoration outcomes, this conclusion was obtained after only one year of surveying, which is much faster than one would expect in order to observe significant differences in channel dimensions.

The picture of sediment transport that this study provides, however, is complicated by the occurrence of at least three bedload transport conditions. The first is commonly known as partial mobility and is characterized by a negative relation between mobility and particle size. As shown by Wilcock [65], this type of transport is also characterized by a negative relation between transport distance and particle size. This description fits the second flooding period in the restoration reach, and

it is for this reason that the overall positive assessment of the restoration outcomes is given. Full mobility, however, which is not characterized by a statistically significant relation between mobility and particle size, can be associated with either a flat or a steep negative power law relation between transport distances and particle size. It is the former condition that is typically called “equal mobility” [65,67], while the latter is the result of unconstrained surface movement of particles over the bed [41]. The occurrence of partial mobility in the restoration reach and the contrast with the control reach could thus be explained by the surface roughness of the constructed riffles, which may be modulating the transport and entrainment of particles at the bed surface. Over time, the large pore spaces of this non-alluvial material may be reduced due to infilling, and the contrast of sedimentary responses between the reaches may be similarly reduced.

One area of significant uncertainty in design is the sensitivity of sediment dynamics to pool-riffle morphology. This widely used analog from natural gravel bed rivers is known to result in spatial differences in particle imbrication [68], routing [69,70], and mean and turbulent shear stresses [45,71]. It is difficult to determine exactly why these differences arise or why they might be important for riffle-pool formation and maintenance, which is likely why debate on the subject has persisted for so long. While a full examination of the debate is beyond the scope of this article, the entrainment of particles in the pool does indicate that shear stresses are sufficient to move gravel particles out of this location while they remain stable in other locations. Similar results have been found in a forced pool [45]. Particle interactions may again be useful for explaining the different behavior as the surface material was much coarser in the constructed riffle than in the pool. Lateral differentiation of deposition by particle size in the pool follows what has been found in channel meanders and is thought to be related to secondary circulation and reduced stresses at the inside of the bed [72]. Deposition in riffles follows what has been found in other systems at high flows [73] and could be related to the trapping of particles within the angular material used in the constructed riffle. Regardless of the precise mechanisms, it is clear that sediment transport predictions should be themselves sensitive to morphology. Predictions of mobility or transport rates based on equations that do not take morphology into consideration cannot address spatial variability.

Our results also illustrate the need for a careful consideration of sample size and seeding strategy in the design of monitoring projects. Statistical tests were implemented as a direct response to Wilcock’s [2] call for quantified and testable hypotheses, but the current study also used some conventions from past work, for example by tracking a large number of particle size classes with relatively small samples for each class. This approach resulted in large error bars on mobility plots (Figure 9), which reduced the ability to distinguish between reaches. From Equation (5), it can be shown that the confidence intervals (assuming a sample mobility of 0.50) are ± 0.22 if the sample size is 20 particles, while 100 particles or more are necessary to reduce the confidence intervals to less than ± 0.10 . Larger sample sizes in fewer size classes are more likely to distinguish differences in mobility between reaches. Additional variability occurs as a result of morphology and the lateral position of the tagged particles relative to the thalweg position (Figures 7 and 8). Variability could be reduced by seeding particles in areas such as the thalweg and in riffles where spatial variability of entrainment is lower. A final consideration is the placement of the particles on the bed. The strategy of loose seeding is advantageous because it isolates the effect of fluid shear stress on entrainment from that of particle interactions such as imbrication. However, it does tend to result in a power law distribution for travel distances instead of

the curved relation expected for gravel beds in partial mobility [41,65]. Accurate estimates of travel distance distributions, particularly in the initial floods after seeding, would thus necessitate a method of particle replacement where tagged particles are placed within the surface and/or subsurface matrix of particles.

5. Conclusions

The foregoing results and discussion support the following conclusions:

1. Using appropriate statistical techniques, sediment tracking can be applied to compare sediment dynamics in restored and control channels as a means of assessing the effectiveness of stream restoration projects;
2. The particular results of this field study demonstrate success in the sense that sediment dynamics are positively affected by the pool-riffle design. Particles in motion tend to be trapped in riffles and the mobility of larger particle sizes is reduced in comparison with a control reach even as the smaller material is scoured from the pool and transported downstream into point bars and the channel margins;
3. Careful attention should be paid to sample sizes and seeding strategies in order to maximize the ability of the sediment tracking approach to distinguish differences in the sediment dynamics between reaches.

The main advantage of the described approach is that stable, degraded, and restored reaches can be placed in a continuum of sediment supply and transport. This advantage significantly advances our ability to manage rivers because it links restoration with sediment supply and transport, which is a critical gap in the planning and analysis of many existing projects. Continued monitoring of sediment dynamics and topographic changes are recommended to assess the design over a longer time period.

Acknowledgments

The authors would like to thank the four reviewers for their detailed and insightful comments that improved an earlier version of this manuscript. The authors are indebted to our partners on this project including Bill Snodgrass at the City of Toronto, Ryan Ness and Christine Tu at the Toronto Region Conservation Authority, and John Parish at Parish Geomorphic Ltd. (now Matrix Solutions Ltd.). This project would not have been possible without their support. Margot Chapuis and Emma Buckrell were partially supported through an NSERC ENGAGE grant with Parish Geomorphic. Funding was also supplied through NSERC Discovery Grants to the first and last authors.

Author Contributions

Bruce MacVicar, Margot Chapuis and André Roy conceived and designed the field experiment, Margot Chapuis and Emma Buckrell installed the equipment and collected the data, Bruce MacVicar, Margot Chapuis and Emma Buckrell analyzed the data, Margot Chapuis and Emma Buckrell wrote and presented preliminary work used for the paper, Bruce MacVicar wrote the paper, Margot Chapuis and André Roy edited the paper.

Conflicts of Interest

The authors declare no conflict of interest.

References

1. Shields, F.D.; Copeland, R.R.; Klingeman, P.C.; Doyle, M.W.; Simon, A. Design for stream restoration. *J. Hydraul. Eng.* **2003**, *129*, 575–584.
2. Wilcock, P.R. Stream restoration in Gravel-Bed Rivers. In *Gravel-Bed Rivers VII*; Church, M., Biron, P., Roy, A.G., Eds.; Wiley: Tadoussac, QC, Canada, 2012; pp. 137–146.
3. Wohl, E.; Angermeier, P.L.; Bledsoe, B.; Kondolf, G.M.; MacDonnell, L.; Merritt, D.M.; Palmer, M.A.; Poff, N.L.; Tarboton, D. River restoration. *Water Resour. Res.* **2005**, *41*, doi:10.1029/2005WR003985.
4. Bernhardt, E.S.; Palmer, M.A.; Allan, J.D.; Alexander, G.; Barnas, K.; Brooks, S.; Carr, J.; Clayton, S.; Dahm, C.; Follstad-Shah, J.; *et al.* Synthesizing US river restoration efforts. *Science* **2005**, *308*, 636–637.
5. Slate, L.O.; Shields, D.F.; Schwartz, J.S.; Carpenter, D.D.; Freeman, G.E. Engineering design standards and liability for stream channel restoration. *J. Hydraul. Eng.* **2007**, *133*, 1099–1102.
6. Radspinner, R.R.; Diplas, P.; Lightbody, A.F.; Sotiropoulos, F. River training and ecological enhancement potential using in-stream structures. *J. Hydraul. Eng.* **2010**, *136*, 967–980.
7. Downs, P.W.; Kondolf, G.M. Post-project appraisals in adaptive management of river channel restoration. *Environ. Manag.* **2002**, *29*, 477–496.
8. Kondolf, G.M.; Anderson, S.; Lave, R.; Pagano, L.; Merenlender, A.; Bernhardt, E.S. Two decades of river restoration in California: What can we learn? *Restor. Ecol.* **2007**, *15*, 516–523.
9. Bernhardt, E.S.; Sudduth, E.B.; Palmer, M.A.; Allan, J.D.; Meyer, J.L.; Alexander, G.; Follstad-Shah, J.; Hassett, B.; Jenkinson, R.; Lave, R.; *et al.* Restoring rivers one reach at a time: Results from a survey of U.S. river restoration practitioners. *Restor. Ecol.* **2007**, *15*, 482–493.
10. Miller, J.R.; Kochel, R.C. Assessment of channel dynamics, in-stream structures and post-project channel adjustments in North Carolina and its implications to effective stream restoration. *Environ. Earth Sci.* **2009**, *59*, 1681–1692.
11. Shields, F.D., Jr. Do we know enough about controlling sediment to mitigate damage to stream ecosystems? *Ecol. Eng.* **2009**, *35*, 1727–1733.
12. Morandi, B.; Piégay, H.; Lamouroux, N.; Vaudor, L. How is success or failure in river restoration projects evaluated? Feedback from french restoration projects. *J. Environ. Manag.* **2014**, *137*, 178–188.
13. Chin, A. Urban transformation of river landscapes in a global context. *Geomorphology* **2006**, *79*, 460–487.
14. Bernhardt, E.S.; Palmer, M.A. Restoring streams in an urbanizing world. *Freshw. Biol.* **2007**, *52*, 738–751.
15. Lacey, J.; Millar, R.G. Reach scale hydraulic assessment of instream salmonid habitat restoration. *J. Am. Water Resour. Assoc.* **2004**, *40*, 1631–1644.

16. Sear, D.A.; Newson, M.D. The hydraulic impact and performance of a lowland rehabilitation scheme based on pool-riffle installation: The River Waveney, Scole, Suffolk, UK. *River Res. Appl.* **2004**, *20*, 847–863.
17. Brown, R.A.; Pasternack, G.B. Comparison of methods for analysing salmon habitat rehabilitation designs for regulated rivers. *River Res. Appl.* **2009**, *25*, 745–772.
18. Abad, J.D.; Rhoads, B.L.; Güneralp, I.; García, M.H. Flow structure at different stages in a meander-bend with bendway weirs. *J. Hydraul. Eng.* **2008**, *134*, 1052–1063.
19. MacWilliams, J.M.L.; Tompkins, M.R.; Street, R.L.; Kondolf, G.M.; Kitanidis, P.K. Assessment of the effectiveness of a constructed compound channel river restoration project on an incised stream. *J. Hydraul. Eng.* **2010**, *136*, 1042–1052.
20. Paik, J.; Escauriaza, C.; Sotiropoulos, F. Coherent structure dynamics in turbulent flows past in-stream structures: Some insights gained via numerical simulation. *J. Hydraul. Eng.* **2010**, *136*, 981–993.
21. Kang, S.; Sotiropoulos, F. Large-eddy simulation of three-dimensional turbulent free surface flow past a complex stream restoration structure. *J. Hydraul. Eng.* **2015**, doi:10.1061/(ASCE)HY.1943-7900.0001034.
22. Khosronejad, A.; Hill, C.; Kang, S.; Sotiropoulos, F. Computational and experimental investigation of scour past laboratory models of stream restoration rock structures. *Adv. Water Resour.* **2013**, *54*, 191–207.
23. Khosronejad, A.; Kozarek, J.L.; Sotiropoulos, F. Simulation-based approach for stream restoration structure design: Model development and validation. *J. Hydraul. Eng.* **2014**, *140*, doi:10.1061/(ASCE)HY.1943-7900.0000904.
24. Odgaard, A.J.; Spoljaric, A. Sediment control by submerged vanes. *J. Hydraul. Eng.* **1986**, *112*, 1164–1181.
25. Bhuiyan, F.; Hey, R.D.; Wormleaton, P.R. Hydraulic evaluation of W-weir for river restoration. *J. Hydraul. Eng.* **2007**, *133*, 596–609.
26. Bhuiyan, F.; Hey, R.D.; Wormleaton, P.R. Effects of vanes and W-weir on sediment transport in meandering channels. *J. Hydraul. Eng.* **2009**, *135*, 339–349.
27. Jamieson, E.C.; Rennie, C.D.; Townsend, R.D. 3D flow and sediment dynamics in a laboratory channel bend with and without stream barbs. *J. Hydraul. Eng.* **2013**, *139*, 154–166.
28. Kuhnle, R.A.; Alonso, C.V.; Shields, F.D. Local scour associated with angled spur dikes. *J. Hydraul. Eng.* **2002**, *128*, 1087–1093.
29. Thompson, D.M. Channel-bed scour with high versus low deflectors. *J. Hydraul. Eng.* **2002**, *128*, 640–643.
30. Bouska, K.L.; Stoebner, T.J. Characterizing geomorphic change from anthropogenic disturbances to inform restoration in the upper Cache River, Illinois. *J. Am. Water Resour. Assoc.* **2015**, *51*, 734–745.
31. Shields, F.D.; Cooper, C.M.; Knight, S.S. Experiment in stream restoration. *J. Hydraul. Eng.* **1995**, *121*, 494–502.
32. Roni, P.; Beechie, T.J.; Bilby, R.E.; Leonetti, F.E.; Pollock, M.M.; Pess, G.R. A review of stream restoration techniques and a hierarchical strategy for prioritizing restoration in Pacific Northwest watersheds. *North Am. J. Fish. Manag.* **2002**, *22*, 1–20.

33. Roper, B.B.; Konnoff, D.; Heller, D.; Wieman, K. Durability of Pacific Northwest instream structures following floods. *N. Am. J. Fish. Manag.* **1998**, *18*, 686–693.
34. Buchanan, B.P.; Nagle, G.N.; Walter, M.T. Long-term monitoring and assessment of a stream restoration project in central New York. *River Res. Appl.* **2014**, *30*, 245–258.
35. Poff, N.L.; Ward, J.V. Physical habitat template of lotic systems: Recovery in the context of historical pattern of spatiotemporal heterogeneity. *Environ. Manag.* **1990**, *14*, 629–645.
36. Thorp, J.H.; Thoms, M.C.; Delong, M.D. The riverine ecosystem synthesis: Biocomplexity in river networks across space and time. *River Res. Appl.* **2006**, *22*, 123–147.
37. Wilcock, P.R.; McArdell, B.W. Surface-based fractional transport rates: Mobilization thresholds and partial transport of a sand-gravel sediment. *Water Resour. Res.* **1993**, *29*, 1297–1312.
38. Wilcock, P.R.; McArdell, B.W. Partial transport of a sand/gravel mixture. *Water Resour. Res.* **1997**, *33*, 235–245.
39. Haschenburger, J.K.; Wilcock, P.R. Partial transport in a natural gravel bed channel. *Water Resour. Res.* **2003**, *39*, doi:10.1029/2002WR001532.
40. Church, M.; Hassan, M.A. Mobility of bed material in Harris Creek. *Water Resour. Res.* **2002**, *38*, doi:10.1029/2001WR000753.
41. Church, M.; Hassan, M.A. Size and distance of travel of unconstrained clasts on a streambed. *Water Resour. Res.* **1992**, *28*, 299–303.
42. Haschenburger, J.K. Tracing river gravels: Insights into dispersion from a long-term field experiment. *Geomorphology* **2013**, *200*, 121–131.
43. Vázquez-Tarrió, D.; Menéndez-Duarte, R. Bedload transport rates for coarse-bed streams in an Atlantic Region (Narcea River, NW Iberian Peninsula). *Geomorphology* **2014**, *217*, 1–14.
44. Lamarre, H.; MacVicar, B.; Roy, A.G. Using passive integrated transponder (PIT) tags to investigate sediment transport in Gravel-Bed Rivers. *J. Sediment. Res.* **2005**, *75*, 736–741.
45. MacVicar, B.J.; Roy, A.G. Sediment mobility in a forced riffle-pool. *Geomorphology* **2011**, *125*, 445–456.
46. Liébault, F.; Bellot, H.; Chapuis, M.; Klotz, S.; Deschâtres, M. Bedload tracing in a high-sediment-load mountain stream. *Earth Surf. Process. Landf.* **2012**, *37*, 385–399.
47. Bradley, N.D.; Tucker, G.E. Measuring gravel transport and dispersion in a mountain river using passive radio tracers. *Earth Surf. Process. Landf.* **2012**, *37*, 1034–1045.
48. Schneider, J.M.; Turowski, J.M.; Rickenmann, D.; Hegglin, R.; Arrigo, S.; Mao, L.; Kirchner, J.W. Scaling relationships between bed load volumes, transport distances, and stream power in steep mountain channels. *J. Geophys. Res. Earth Surf.* **2014**, *119*, 533–549.
49. Chapuis, M.; Dufour, S.; Provansal, M.; Couvert, B.; de Linares, M. Coupling channel evolution monitoring and RFID tracking in a large, wandering, gravel-bed river: Insights into sediment routing on geomorphic continuity through a riffle-pool sequence. *Geomorphology* **2015**, *231*, 258–269.
50. Houbrechts, G.; Levecq, Y.; Peeters, A.; Hallot, E.; van Campenhout, J.; Denis, A.C.; Petit, F. Evaluation of long-term bedload virtual velocity in gravel-bed rivers (Ardenne, Belgium). *Geomorphology* **2015**, doi:10.1016/j.geomorph.2015.05.012.

51. Arnaud, F.; Piégay, H.; Vaudor, L.; Bultingaire, L.; Fantino, G. Technical specifications of low-frequency radio identification bedload tracking from field experiments: Differences in antennas, tags and operators. *Geomorphology* **2015**, *238*, 37–46.
52. Biron, P.M.; Carver, R.B.; Carré, D.M. Sediment transport and flow dynamics around a restored pool in a fish habitat rehabilitation project: Field and 3D numerical modelling experiments. *River Res. Appl.* **2011**, *28*, 926–939.
53. Krapesch, G.; Tritthart, M.; Habersack, H. A model-based analysis of meander restoration. *River Res. Appl.* **2009**, *25*, 593–606.
54. Habersack, H.; Jäger, E.; Hauer, C. The status of the Danube River sediment regime and morphology as a basis for future basin management. *Int. J. River Basin Manag.* **2013**, *11*, 153–166.
55. Chapuis, M.; Bright, C.J.; Hufnagel, J.; Macvicar, B. Detection ranges and uncertainty of passive radio frequency identification (RFID) transponders for sediment tracking in gravel rivers and coastal environments. *Earth Surf. Process. Landf.* **2014**, *39*, 2109–2120.
56. Parish Geomorphic. TRCA Wilket Creek Emergency Works (Sites 6&7)—Technical Design Brief. Available online: <http://trca.on.ca/the-living-city/green-infrastructure-projects/environmental-assessment-projects/wilket-creek-rehabilitation-project.dot>. (accessed on 14 October 2015)
57. Bevan, V. The Effect of Urbanisation on Sediment Supply and Transport: A Field Study of Wilket Creek in Toronto. Master's Thesis, University of Waterloo, Waterloo, ON, Canada, 28 August 2014; p. 157.
58. Heritage, G.L.; Milan, D.J.; Large, A.R.G.; Fuller, I.C. Influence of survey strategy and interpolation model on DEM quality. *Geomorphology* **2009**, *112*, 334–344.
59. Parker, G. Transport of gravel and sediment mixtures. In *Sedimentation Engineering: Processes, Management, Modeling, and Practice*; Garcia, M.H., Ed.; ASCE: Reston, VA, USA, 2008; pp. 165–252.
60. Buffington, J.M.; Montgomery, D.R. A systematic analysis of eight decades of incipient motion studies with special reference to gravel-bedded rivers. *Water Resour. Res.* **1997**, *33*, 1993–2029.
61. Collett, D. *Modelling Binary Data*, 2nd ed.; Chapman and Hall/CRC: Boca Raton, FL, USA, 2002; p. 387.
62. Wald, A.; Wolfowitz, J. On a test whether two samples are from the same population. *Ann. Math. Stat.* **1940**, *11*, 147–162.
63. Goddard, S.D.; Genton, M.G.; Hering, A.S.; Sain, S.R. Evaluating the impacts of climate change on diurnal wind power cycles using multiple regional climate models. *Environmetrics* **2015**, *26*, 192–201.
64. Fonseca, M.S.; Kenworth, W.J.; Griffith, E.; Hall, M.O.; Finkbeiner, M.; Bell, S.S. Factors influencing landscape pattern of the seagrass *Halophila decipiens* in an oceanic setting. *Estuar. Coast. Shelf Sci.* **2008**, *76*, 163–174.
65. Wilcock, P.R. Entrainment, displacement and transport of tracer gravels. *Earth Surf. Process. Landf.* **1997**, *22*, 1125–1138.
66. Ferguson, R.I.; Bloomer, D.J.; Hoey, T.B.; Werritty, A. Mobility of river tracer pebbles over different timescales. *Water Resour. Res.* **2002**, *38*, doi:10.1029/2001WR000254.
67. Parker, G.; Klingeman, P.C.; MacLean, D.G. Bedload and size distribution in paved gravel-bed streams. *J. Hydraul. Div.* **1982**, *108*, 544–571.

68. Sear, D.A. Sediment transport processes in pool-riffle sequences. *Earth Surf. Process. Landf.* **1996**, *21*, 241–262.
69. MacWilliams, M.L.J.; Wheaton, J.M.; Pasternack, G.B.; Street, R.L.; Kitanidis, P.K. Flow convergence routing hypothesis for pool-riffle maintenance in alluvial rivers. *Water Resour. Res.* **2006**, *42*, doi:10.1029/2005WR004391.
70. Milan, D.J. Sediment routing hypothesis for pool-riffle maintenance. *Earth Surf. Process. Landf.* **2013**, *38*, 1623–1641.
71. Thompson, D.M.; Wohl, E.E. The linkage between velocity patterns and sediment entrainment in a forced-pool and riffle unit. *Earth Surf. Process. Landf.* **2009**, *34*, 177–192.
72. Bridge, J.S.; Jarvis, J. The dynamics of a river bend: A study in flow and sedimentary processes. *Sedimentology* **1982**, *29*, 499–541.
73. Jackson, W.L.; Beschta, R.L. A model of two-phase bedload transport in an Oregon coast range stream. *Earth Surf. Process. Landf.* **1982**, *7*, 517–527.

© 2015 by the authors; licensee MDPI, Basel, Switzerland. This article is an open access article distributed under the terms and conditions of the Creative Commons Attribution license (<http://creativecommons.org/licenses/by/4.0/>).